*Journal of Sound and Vibration* (2000) **231**(4), 1135–1157
doi:10.1006/jsvi.1999.2724, available online at http://www.idealibrary.com on IDEAL®

# A THEORETICAL AND COMPUTATIONAL STUDY OF THE FRF-BASED SUBSTRUCTURING TECHNIQUE APPLYING ENHANCED LEAST SQUARE AND TSVD APPROACHES

T. C. LIM

*Department of Mechanical Engineering*, 290 *Hardaway Hall*, *Box* 870276, *The University of Alabama*, *Tuscaloosa*, *AL* 35487-0276, *U.S.A.*

AND

J. LI

*Center for Automotive Research*, *The Ohio State University*, 930 *Kinnear Road*, *Columbus*, *OH* 43212, *U.S.A.*

(*Received* 19 *November* 1998, *and in final form* 22 *September* 1999)

The frequency response function (FRF)-based substructuring technique has been previously proposed for computing the vibratory response of complex built-up structures with moderately high-modal density characteristic. This is because it has the advantage of being able to incorporate experimental component FRFs directly into its spectral formulation. However, the accuracy of this technique is frequently hindered by spectral distortion problem due to amplification of errors in the FRF-matrix during an inversion calculation. To analyze the influence of error amplification, its inherent FRF-matrix inverse problem is mathematically transformed into an over-determined set of linear algebraic equations. The least-squares (LS) and total least-squares (TLS) solution schemes are proposed to handle this new formulation. It is then shown that these two proposed algorithms can lead to some improvements in the predictions but cannot eliminate the influence of error completely. To further achieve more accurate dynamic coupling response, the truncated singular value decomposition (TSVD) scheme is proposed to work in conjunction with the LS and TLS algorithms. Its effectiveness in reducing the influence of pre-existing errors in the FRF-matrix when applying this type of substructuring technique to a two-component system is investigated theoretically and computationally. This study also led to the discovery of certain new condition under which the TSVD scheme is most effective.



## 1. INTRODUCTION

The dynamic characteristic of complex built-up structures are usually difficult to model either analytically or experimentally. Since it is generally easier and more accurate to formulate the dynamic response of simpler components, numerous researchers [1–9] have proposed using dynamically coupled component models to

0022-460X/00/141135 + 23 $35.00/0 

predict the vibratory behavior of highly complex structures. Among some of the notable dynamic coupling techniques, the frequency response function (FRF)-based substructuring technique [3–9] is found to be a rather convenient and attractive method for computing the response spectra of linear and quasi-linear structural systems. The fundamental concept of this technique is to utilize individual uncoupled component FRFs to construct the total system response via either an impedance or compliance-type computational equation. This method does not require a knowledge of the system modes that can be very difficult to compute accurately especially for higher order ones. Moreover, it has all the advantages of being able to incorporate experimentally measured component FRFs directly into the formulation, which tend to have higher frequency limitations compared to analytical-based computational models. For instance, Ochsner and Bernhard [4] used this modelling techniques to analyze the structure-borne noise transmission from the tyre spindle, through the suspension, and into the passenger compartment of an automobile. The FRFs of each component used in their calculations are measured directly from component set-ups, and the bushing connectors are modelled as simple spring–damper elements. Lim and Steyer [5, 6] also applied a variation of this method by using experimental FRFs of a moderately high-modal density body component to analyze some specific automotive noise and vibration problems, and also ultimately obtained reasonably good results even though a number of modelling iterations were needed.

In spite of several promising success reported in the literature, one of the major computational difficulties of this type of analysis, which inherently requires several matrix inversion calculations, is the amplification of errors in the experimental FRF-matrix inversion process. The computation can lead to not only significant spectral response distortion but also generation of spurious peaks in the predicted response spectra [7–9]. Thus, there is a need to obtain a better understanding of the influence of component FRF errors on system response spectra, and also develop a robust computational approach that minimizes this effect when applying the proposed FRF-based substructuring technique for prediction of the higher frequency vibratory response.

In recent studies of FRF-based component synthesis technique by Lim and Steyer [5–7] and Otte *et al.* [8, 9] as mentioned above, the truncated singular value decomposition (TSVD) scheme was used in an attempt to overcome the computational deficiency of this approach in the presence of measurement error as opposed to the statistical method discussed in references [10, 11]. The basic idea here is to nullify the smallest set of singular values belonging to the experimental FRF-matrix, which are believed to be highly sensitive to the presence of measurement errors. In a much earlier but unrelated study [12], this TSVD concept was actually applied to achieve numerical stability due to computational round-off error. Later, this idea was adopted to deal with noisy measurement data in numerous inverse and identification problems on vibrations of structures such as the study performed by Powel [13]. In a subsequent effort by Lim and Steyer [5–7] involving a high modal density and damping system, they repeatedly showed that it is possible to achieve relatively accurate spectra if a proper set of filtering levels, which was derived by trial-and-error, is used. No specific criterion for the threshold

limit of the singular values is suggested. In addition, their work did not provide a thorough analysis of the effectiveness of TSVD, hence making it quite difficult to apply this technique without prior knowledge of the precise system response. At about the same time, Otte *et al.* [8, 9] also worked on a compliance formulation using TSVD, and applied it semi-empirically in spatial and frequency domains to perturbed analytical components. Similarly, their studies also did not provide an in-depth treatment of the effect of TSVD when applied to component synthesis approach using component response spectra. This has contributed to, not only an incomplete understanding of the effect of TSVD in component dynamic coupling, but lack of any criterion for the handling of the singular values.

It is the objective of this paper to address these issues theoretically and computationally. First, we will show that the problem of analyzing the influence of measured or computed FRF errors on system response in the FRF-based component synthesis technique can be mathematically transformed into the equivalent problem of studying the numerical stability of an over-determined set of linear algebraic equations. Two solution schemes are proposed and examined in detail: the least-squares (LS) and total least-squares (TLS) algorithms. Then to further achieve better predictions, the TSVD scheme is integrated with the LS and TLS algorithms, and their combined predictions are compared to theoretical results to investigate the effectiveness in minimizing the influence of errors in the FRF-matrix. This study also reveals certain conditions in which the TSVD algorithm can be applied effectively.

## 2. FRF-BASED SYNTHESIS FORMULATION

Consider a two-component structural system, as depicted in Figure 1. Each component comprises of $n$ discrete unidirectional interface connections denoted by subscript $i$. The connections can be either rigid or flexible with dynamic stiffness

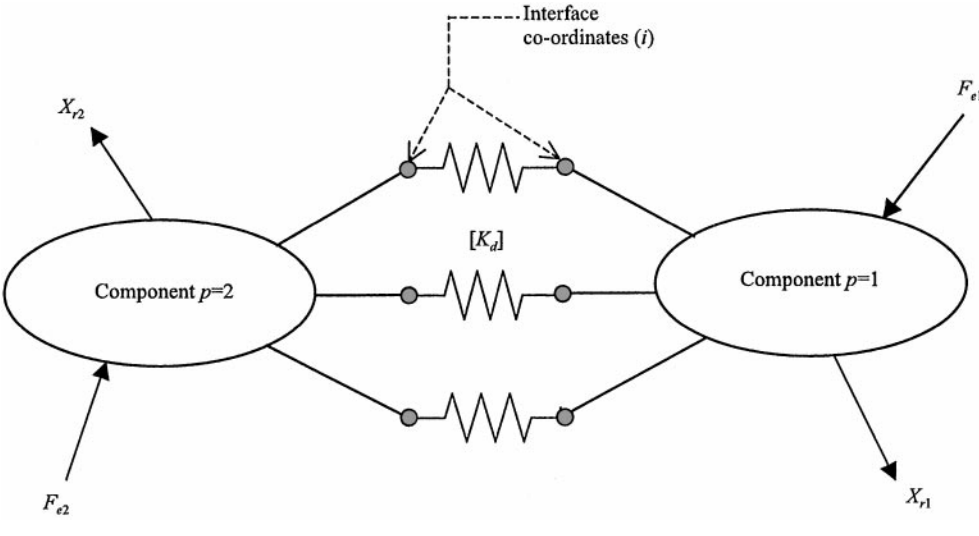


Figure 1. A symbolic illustration of the coupling of a two-component system.

characteristic given by $[K_d]$ that varies with frequency. Each element in $[K_d]$ is generally complex valued since each connector is represented as a spring–damper set. However, it can be reduced to real valued if the connection is simply regarded as a pure spring element. Assuming that the uncoupled component FRF-matrix $[H_{iip}]$ for the interface coupling co-ordinates, and transfer functions from the coupling points to the response and excitation co-ordinates given by $\{H_{rip}\}$ and $\{H_{iep}\}$, respectively, are known precisely, one can show that the general linear structural system response function denoted by subscript $S$, based on dynamic compliance formulation, can be expressed as

$$(X_{rp}/F_{eq})_S = \delta_{pq} H_{rep} + \gamma_{pq} \{H_{rip}\}^H ([H_{ii1}] + [H_{ii2}] + [K_d]^{-1})^{-1} \{H_{ieq}\}, \quad (1a)$$

$$\delta_{pq} = \begin{cases} 1, & p = q \\ 0, & p \neq q \end{cases}, \quad \gamma_{pq} = \begin{cases} -1, & p = q \\ +1, & p \neq q \end{cases}, \quad (1b,c)$$

which is compatible with the formulation used in previous studies [4–9]. It can be seen clearly in the above equation that the system response function $(X_{rp}/F_{eq})_S$ inherently requires an inversion of the superposition of three compliance matrices related to the coupling terms. This represents a potential source of error amplification. Also, since the system response is largely determined by $[H_{ii1}] + [H_{ii2}] + [K_d]^{-1}$, this matrix could be regarded as the "virtual" compliance matrix of the combined structural system.

For problems involving vibratory energy transfer from one component to another, which is of primary interest here, one typically deals with the case of $p \neq q$ where $p, q \in \{1, 2\}$. In this case, $X_{rp}$ does not reside in the same component where the external excitation $F_{eq}$ is applied. Also, if the coupling stiffness terms are included as part of one component, then equation (1) can be rewritten, without loss of generality, as

$$(X_{rp}/F_{eq})_S = \{H_{rip}\}^H [H_{iip}]^{-1} [H_{iiS}] \{R_{ieq}\}, \quad (2)$$

where $[H_{iiS}] = ([H_{ii1}]^{-1} + [H_{ii2}]^{-1})^{-1}$ is the true system compliance matrix for the coupling co-ordinates, and $\{R_{ieq}\} = [H_{iiq}]^{-1} \{H_{ieq}\}$ is the component force transmissibility function from the excitation point to the coupling co-ordinates as if the interface is rigidly constrained to be motionless. Note that the same formulation is obtained if $[K_d]^{-1} \ll [H_{iip}]$. The resultant equation is most suitable for predicting system response on an experimental component $p$ due to excitation force applied to an analytical component $q$, because $\{R_{ieq}\}$ can be easily computed directly while $\{H_{rip}\}$ and $[H_{iip}]$ can be measured given the specific component hardware. Also, it may be noted that $[H_{iiS}]\{R_{ieq}\}$ physically relates to the system vibratory response at the coupling co-ordinates due to $F_{eq}$. Its product with $[H_{iip}]^{-1}$, as given by the last three terms in equation (2), is the system level dynamic loads transmitted across the discrete coupling connections. On the surface, equation (2) looks more cumbersome due to the additional layer of the matrix inverse in $[H_{iiS}]$, however, it is in fact better suited for the application of TSVD proposed in this study as we shall see later in this article.

The basis for successful application of equations (1) and (2) above lies in the accuracy of the matrix inversions since the other terms are typically easier to

compute. A detailed look at this numerical issue is given next. In general, the discrepancies in $[H_{ii1}]$ and $[H_{ii2}]$ may be different because they come from two different sources and components, especially when one is measured experimentally and the other is computed analytically by means of methods like finite elements, for instance. In this study, we are most interested in examining the case in which most of the error quantities are clustered in only one set of component FRF, say $[H_{iip}]$. To better deal with this problem, we need to understand the effect of total error amplification in calculation of $[H_{iip}]^{-1}[H_{iiS}] = [H_1]$. For subscript $p = 1$ or 2 (where the subscript $p$ indicates the component whose FRFs are inaccurate), $[H_1]$ can be shown to be equivalent to

$$[H_1] = [I_n] - [X], \quad [X] = ([H_{ii1}] + [H_{ii2}])^{-1}[H_{iip}], \tag{3a,b}$$

where $[I_n]$ is the identity matrix of dimension $n$. If equation (3b) is premultiplied by $[H_{ii1}] + [H_{ii2}] = [A]$, we obtain a set of linear algebraic equations in matrix form as

$$[A][X] = [B], \tag{4}$$

where $[B] = [H_{iip}]$ and $[X]$ is the solution to this linear algebraic problem. Obviously, the accuracy of computed $[X]$ determines that of $[H_1]$. With this transformation, the problem of observing the effect of error amplification and distortion on system response spectra becomes the problem of analyzing the solution to a set of linear algebraic equations whose matrix coefficients $[A]$ and $[B]$ are perturbed from their theoretical values. This viewpoint had not been proposed in the past even though it has many advantages over the direct formulations shown in equations (1) and (2). In addition, the importance of deriving equation (4) also lies in the fact that it provides more flexibility to deal with measurement error in the component FRFs. This is because equation (4) can be set-up to be over-determined resulting in the problem of $[\tilde{A}][\tilde{X}] = [\tilde{B}]$, where both $[\tilde{A}]$ and $[\tilde{B}]$ are $m \times n$ matrices ($m > n$) when more than one set of $[H_{iip}]$ of dimension $n$ is available. Here, the symbol $\sim$ is used to indicate that the matrices have been compromised by error. Accordingly, $[\tilde{A}] = [A] + [E_A]$ and $[\tilde{B}] = [B] + [E_B]$, where $[E_A]$ and $[E_B]$ represent the error matrices. For such an error-in-variable multivariate model, a variety of spectral curve-fitting techniques for estimating the unknown parameters can be applied. In theory, for systems with zero-mean and independent error, the true and consistent estimate of $[X]$ can be computed as $m$ approach infinity [14]. However, in practice, one can only use a finite $m$. Also, since $[H_1]$ is the core FRF matrix for determining system response spectra as shown in equation (2), one can easily compute the dynamic response at any point denoted by subscript $r$ given a relatively good estimate of $[H_1]$.

## 3. LS AND TLS SOLUTION SCHEMES

### 3.1. FORMULATION

Since $[X]$ and $[B]$ are essentially matrices, the problem posed by equation (4) can be regarded as a grouping of a series of the more classical algebraic equation set of the form $[A]\{x\} = \{b\}$. Each set of algebraic equations has identical $[A]$ matrix,

but differs in $\{b\}$, which represents the individual column vectors of $[B]$. For each algebraic problem, $\{x\}$ can be computed from either the least-squares (LS) or total least-squares (TLS) algorithm as described below.

According to the theorem of SVD, any $m \times n$ matrix $[A]$ in the complex field can be decomposed exactly as $[A] = [U][\Lambda][V]^H$, where the left and right matrices $[U] \in C^{m \times m}$ and $[V] \in C^{n \times n}$ are unitary matrices span by complex space $C$, and $[\Lambda] \in R^{m \times n}$ is a diagonal matrix of singular values in form of $[\Lambda] = \text{diag}(s_1, s_2, \ldots, s_w, 0 \cdots 0)$ where $s_1 > s_2 > \cdots > s_w$. The subscript $w$ denotes the rank of $[A]$. It is reasonable to assume that $w = n$ in this paper since it is very unlikely that the det($[A]$) in equation (4) is identically zero. This is due to the fact that factors like geometrical approximation, measurement error and damping effect of the structural system would cause enough variation in $[A]$ to prevent it from being singular. Since matrix $[A] = [H_{ii1}] + [H_{ii2}]$ is the "virtual" compliance matrix of the coupled system,the column vectors in $[U]$ are directly related to the spatial deformations of the structural system at the interface span by the orthogonal eigenspace, and $[\Lambda]$ is the "virtual" compliance matrix corresponding to these eigenco-ordinate vectors. Accordingly, a small singular value qualitatively refers to a dynamically stiff structural coupling corresponding to the specific eigenvector displacement.

Accordingly, $[A]^{-1}$ can be determined from the Moore–Penrose pseudo-inverse defined as $[A]^+ = [\text{V}][\Lambda]^+[U]^H$, where $[\Lambda] = \text{diag}(1/s_1, 1/s_2, \ldots, 1/\text{s}_n]$ comprises of the reciprocal of the singular values of $[A]$. In this theorem, $\{x\} = [A]^+\{b\}$ actually gives the unique solution that minimizes the second norm of $\{x\}$ denoted by $\|\{x\}\|_{II}$ where the mathematical condition of $\{x\} \in \{\{x\}; \|[A]\{x\} - \{b\}\|_{II} = \min\}$ is satisfied [15]. Therefore, the extended LS solution to the problem posed by equation (4) is given in terms of $[X_{LS}] = [A]^+[B]$.

In the LS scheme described above, only $[B]$ is assumed to deviate from its theoretical state because the method strictly minimizes the error variation in $[B]$. However, in our actual problem, both $[A]$ and $[B]$ are subjected to the same measurement error contained in $[H_{iip}]$. To consider the influence of these error variations in $[A]$ and $[B]$ simultaneously, the TLS scheme is proposed as an alternative solution because it can be used to minimize the Frobenious norm $\|[\Delta A][\Delta B]\|_F$, while imposing the mathematical condition of Range $([B] - [\Delta B]) \subseteq$ Range $([A] - [\Delta A])$. Here, Range($[P]$) represents the column vector space of matrix $[P]$. Therefore, the total least-squares solution $[X_{TLS}]$ is determined by solving $([A] - [\Delta A])[X_{TLS}] = [B] - [\Delta B]$.

Suppose that the solution to $[\tilde{A}][\tilde{X}] = [\tilde{B}]$ exists. In order to solve for $[\tilde{X}]$, the problem is first rewritten as

$$[[\tilde{A}][\tilde{B}]] \begin{Bmatrix} [\tilde{X}] \\ -[I] \end{Bmatrix} = 0. \tag{5}$$

Now, let $[\tilde{C}] = [[\tilde{A}][\tilde{B}]]$, where $[\tilde{C}] = [\tilde{U}][\tilde{\Lambda}][\tilde{V}]^H$, and $[\tilde{U}]$, $[\tilde{\Lambda}]$ and $[\tilde{V}]$ are partitioned as

$$[\tilde{U}] = [[\tilde{U}_a][\tilde{U}_b]], \quad \tilde{\Lambda} = \begin{bmatrix} [\tilde{\Lambda}_a] & 0 \\ 0 & [\tilde{\Lambda}_b] \end{bmatrix}, \quad \tilde{V} = \begin{bmatrix} [\tilde{V}_{aa}] & [\tilde{V}_{ab}] \\ [\tilde{V}_{ba}] & [\tilde{V}_{bb}] \end{bmatrix}, \tag{6}$$

such that $[\tilde{A}] = [\tilde{U}_a][\tilde{\Lambda}_a][\tilde{V}_{aa}]^H + [\tilde{U}_b][\tilde{\Lambda}_b][\tilde{V}_{ab}]^H$ and $[\tilde{B}] = [\tilde{U}_a][\tilde{\Lambda}_a][\tilde{V}_{ba}]^H + [\tilde{U}_b][\tilde{\Lambda}_b][\tilde{V}_{bb}]^H$. Based on the theory of TLS [16, 17], $[[\Delta A]\ [\Delta B]]$ with minimum Frobenious norm is given by $[[\Delta A_0][\Delta B_0]] = [[\tilde{U}_a][\tilde{\Lambda}_b][\tilde{V}_{ab}]^H\ [\tilde{U}_b][\tilde{\Lambda}_b]\ [\tilde{V}_{bb}]^H]$. Subsequently, after removing the minimum norm error matrices, we have a resultant matrix of rank $n$ given by

$$[[\tilde{A}][\tilde{B}]] - [[\Delta A_0][\Delta B_0]] = [[\tilde{U}_a][\tilde{\Lambda}_a][\tilde{V}_{aa}]^H \quad [\tilde{U}_a][\tilde{\Lambda}_a][\tilde{V}_{ba}]^H]. \tag{7}$$

Additionally, if $[\tilde{V}_{bb}]$ is non-singular, then $[\tilde{X}_{TLS}] = -[\tilde{V}_{ab}][\tilde{V}_{bb}]^{-1}$. It is clear that generally $[\Delta A_0] \neq [E_A]$ and $[\Delta B_0] \neq [E_B]$. Although the TLS scheme ideally cannot be used to completely remove all the errors in the FRFs, it can still provide a fairly consistent estimate of $[X]$ if the errors of $[A]$ and $[B]$ are not severe enough and they are identically distributed with zero mean.

Compared to the LS scheme, the TLS intuitively seems better equipped to deal with the error amplification problem. According to the statement made by Van Huffel and Vandewalle [18], if the inequality of $(\tilde{s}_n([\tilde{C}]) - s_{n+1}([C])) > \tilde{s}_n([\tilde{A}])$ is true, then the singular column vector subspaces of $[\tilde{U}([\tilde{C}])]$ and $[\tilde{V}([\tilde{C}])]$ related to the TLS formulation are less noise sensitive than the singular column vector subspaces of $[\tilde{U}([\tilde{A}])]$ and $[\tilde{V}([\tilde{A}])]$ related to the LS scheme. This implies that the TLS singular subspaces are expected to be "closer" to the corresponding unperturbed subspaces of $[[A]\ [B]]$. Accordingly, the TLS solution of $[\tilde{A}][\tilde{X}] = [\tilde{B}]$ is expected to be more accurate than the LS one. When $(\tilde{s}_n([\tilde{C}]) - s_{n+1}([C]))/\tilde{s}_n([\tilde{A}])$ is higher, the advantage of TLS with respect to LS should be even more obvious. This is typically the case when $[\tilde{A}]$ tends to be rank-deficient, that is, $\tilde{s}_n([\tilde{A}]) \approx 0$. Also, when $\tilde{s}_n([\tilde{A}]) > \tilde{s}_{n+1}([\tilde{C}])$ the magnitude difference between the LS and TLS solutions is given by

$$\|[\tilde{X}_{TLS}] - [\tilde{X}_{LS}]\| \leqslant \frac{\tilde{s}_{n+1}^2([\tilde{C}])\|[B]\|}{\tilde{s}_n([\tilde{A}])(\tilde{s}_n^2([\tilde{A}]) - \tilde{s}_{n+1}^2([\tilde{C}]))}. \tag{8}$$

The above equation shows that as $[\tilde{A}]$ tends to be more rank-deficient, $[\tilde{X}_{LS}]$ would deviate farther away from $[\tilde{X}_{TLS}]$. As we have argued that the latter solution is more precise under this condition, the *LS* solution will tend to deviate more from theory at the frequency points where the structural resonances of these components occur. On the other hand, if $\tilde{s}_n([\tilde{A}])$ is large but not close to $\tilde{s}_{n+1}([\tilde{C}])$, the difference between $[\tilde{X}_{TLS}]$ and $[\tilde{X}_{LS}]$ is small. Next two specific numerical cases are analyzed to determine the effects of the proposed solution schemes.

### 3.2. COMPUTATIONAL STUDY

Consider the multi-degrees-of-freedom lumped parameter system with 10 independent interface coupling co-ordinates as illustrated in Figure 2, which is purposely devised to facilitate a systematic and controlled numerical study to precisely quantify the effects of both LS and TLS solution schemes. In this example, we have two components that are dynamically coupled at 10 discrete points. For brevity, only three coupling co-ordinate pairs are shown. When the component FRFs are exact, equation (2) produces the precise response shown in Figure 3(a) as

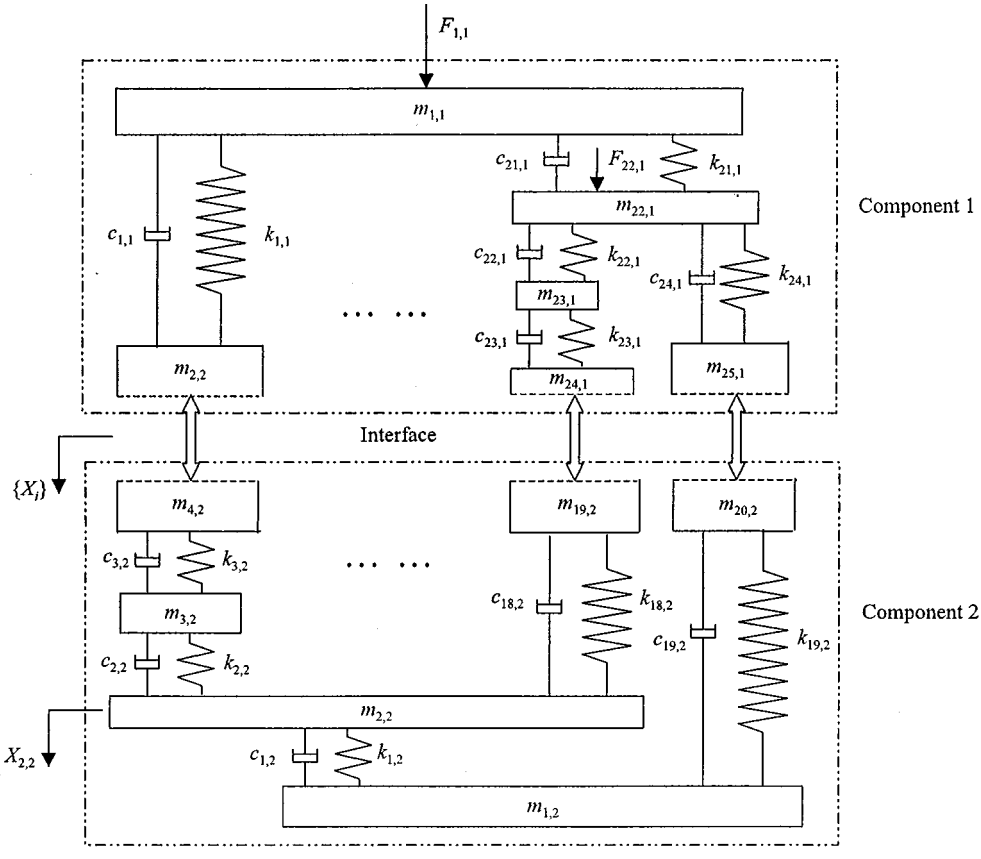


Figure 2. An idealized multi-degrees-of-freedom case consisting of a coupled two-component lumped parameter system model with 10 discrete interface co-ordinates in each component.

predicted by theory. Here, the amplitude response function is given in terms of dB relative to $10^{-5}$ m/s$^2$/N and the phase is in degrees, which are also used consistently throughout this paper.

Next, a random error of no more than 5% of $[H_{iip}]$ is introduced into the component FRFs of $p = 2$. First, the standard direct inversion algorithm is applied assuming that only one set of measured $[H_{ii2}]$ is available, and its computed results are compared to the exact response spectra. A typical comparison is shown in Figure 3(b), where the exact function is represented by a dashed line while the function computed by method of standard direct inverse is given by a solid line. In some frequency range, the coupled response is affected significantly by amplification in the added random errors as one would expect since no special treatment is performed to control the error. For instance, in the frequency range of 2–10 and 12–16 Hz, the true frequency response curve cannot be distinguished clearly due to significant presence of spurious peaks.

Now, suppose two sets of $[H_{ii2}]$ are generated that differ only by the actual added random errors that are again set at less than 5%. Thus, $[A]$ and $[B]$ are now over-determined with dimension $m = 20$ and $n = 10$. Their solutions by means of

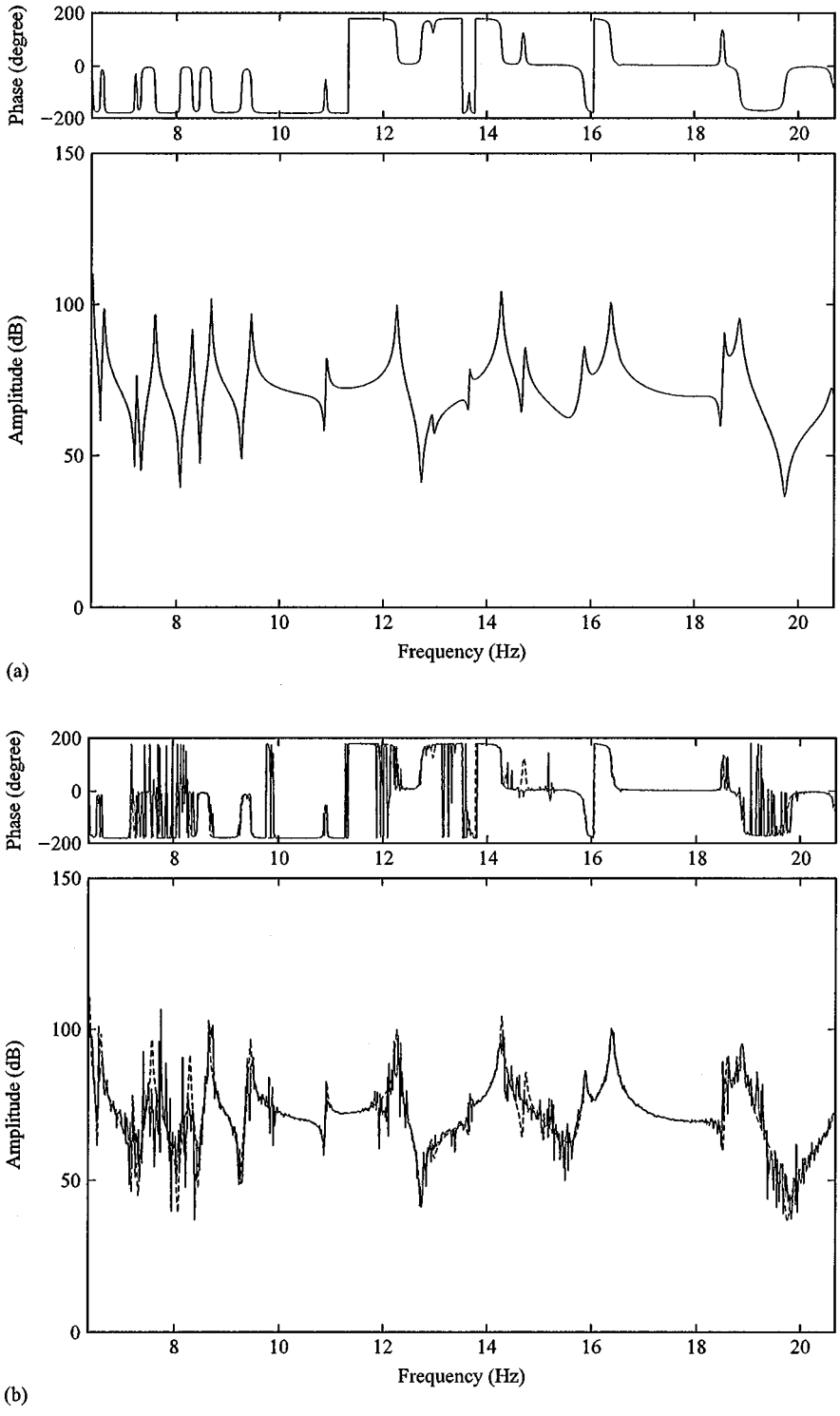


Figure 3. Comparison of exact and predicted system response functions (dB re. $10^{-5}$ m/s$^2$/N) of the two-component lumped parameter model applying the standard direct inverse scheme: (a) no FRF error (– – –, exact; ——, prediction) and (b) with 5% random error (– – –, exact; ——, prediction)

both the LS and TLS algorithms produce $[\tilde{X}_{LS}]$ and $[\tilde{X}_{TLS}]$, respectively, which can be used to recover $[H_I]$ and ultimately the system response of equation (2) through back-substitutions. Typical results are shown in Figures 4(a, b) respectively. The TLS-based prediction generally did better that the LS-based calculation. In the LS-based prediction the resonance amplitudes are off as predicted by theory. Even though both the LS and TLS solutions of the over-determined equation did not succeed in improving the calculated response within 2–10 Hz by very much, they predicted a smoother response curve overall. This implies that the influence of random error amplification manifested by the waviness in the curve has been minimized due to the averaging effect of more than one set of input data. Hence, one would expect the deviation in the predicted response spectra to progressively reduce with increasing $m$. The higher $m$ value will require additional experimental and computational efforts, which can be alleviated by applying greater precision in testing co-ordinate pairs with lowest-quality FRFs. Figure 5 indeed shows that the predicted response spectra of the lumped parameter system (see Figure 2) with $m = 200$ turn out to be much smoother. In spite of this averaging effect, the predicted response is still quite poor in the vicinity of the resonance peaks. This is because there is normally one singular value that dominates the set at the resonance frequencies. The smaller singular values are more susceptible to measurement errors in the LS scheme since $[X_{LS}] = [A]^+[B]$ and $[\Lambda]^+ = \text{diag}(1/s_1, 1/s_2, \ldots, 1/s_n)$. On the other hand, the TLS method does seem to provide a better estimation compared to the LS method under some circumstances as discussed above. This is evident from the comparison of Figures 5(a) and 5(b) where most of the significant resonance peaks are retained in the TLS method.

In the previous idealized case study, both coupled component models are of low-modal density type. It was analyzed to help verify the proposed computational schemes under a controlled setting. Since the FRF-based substructuring technique is most sought after for its ability to utilize experimental FRFs that are particularly suitable for representing the dynamics of the moderately high-modal density component, we now apply the proposed solution schemes to an actual vehicle system as shown in Figure 6. The vehicle body component is attached to a lumped parameter model representing a suspension assembly. In this type of structural system, the FRFs of the higher modal density body component do not show distinct resonant peaks like in the case of the low-modal density substructure. In the former case, the modal response tends to coalesce and damping is high enough to reduce sharpness in the resonance peaks significantly, as discussed quite thoroughly in a previous paper by Lim [5]. Unlike the previous example that deals primarily with random measurement error, this particular problem also contains bias error in the FRFs of the vehicle body component, which further complicates the numerical calculations. The system response at a point on the vehicle body floor panel is computed using the standard direct inverse and the LS solution schemes. In the latter calculation, a set of 20 ($m = 80$) measured compliance FRF-matrices of the vehicle body component is utilized. Their predictions are compared to the exact response within the frequency range of 50–400 Hz in Figure 7(a, b) respectively. The standard direct inverse prediction given in Figure 7(a) clearly shows substantial

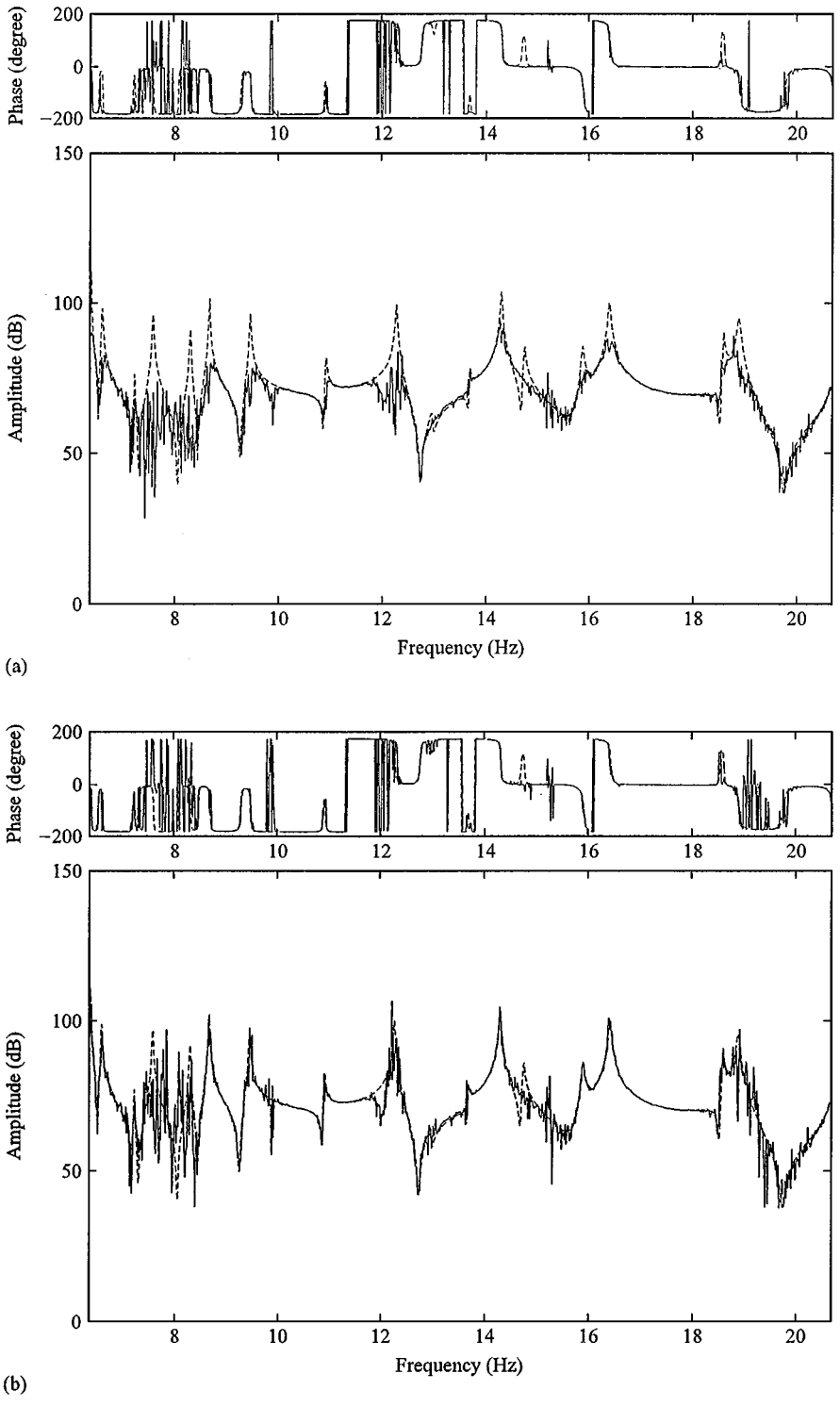


Figure 4. Comparison of exact and predicted system response functions (dB re. $10^{-5}$ m/s$^2$/N) of the two-component lumped parameter model applying LS and TLS algorithms with $m = 20$: (a) LS solution scheme (– – –, exact; —— prediction) and (b) TLS solution scheme (– – –, exact; ——, prediction).

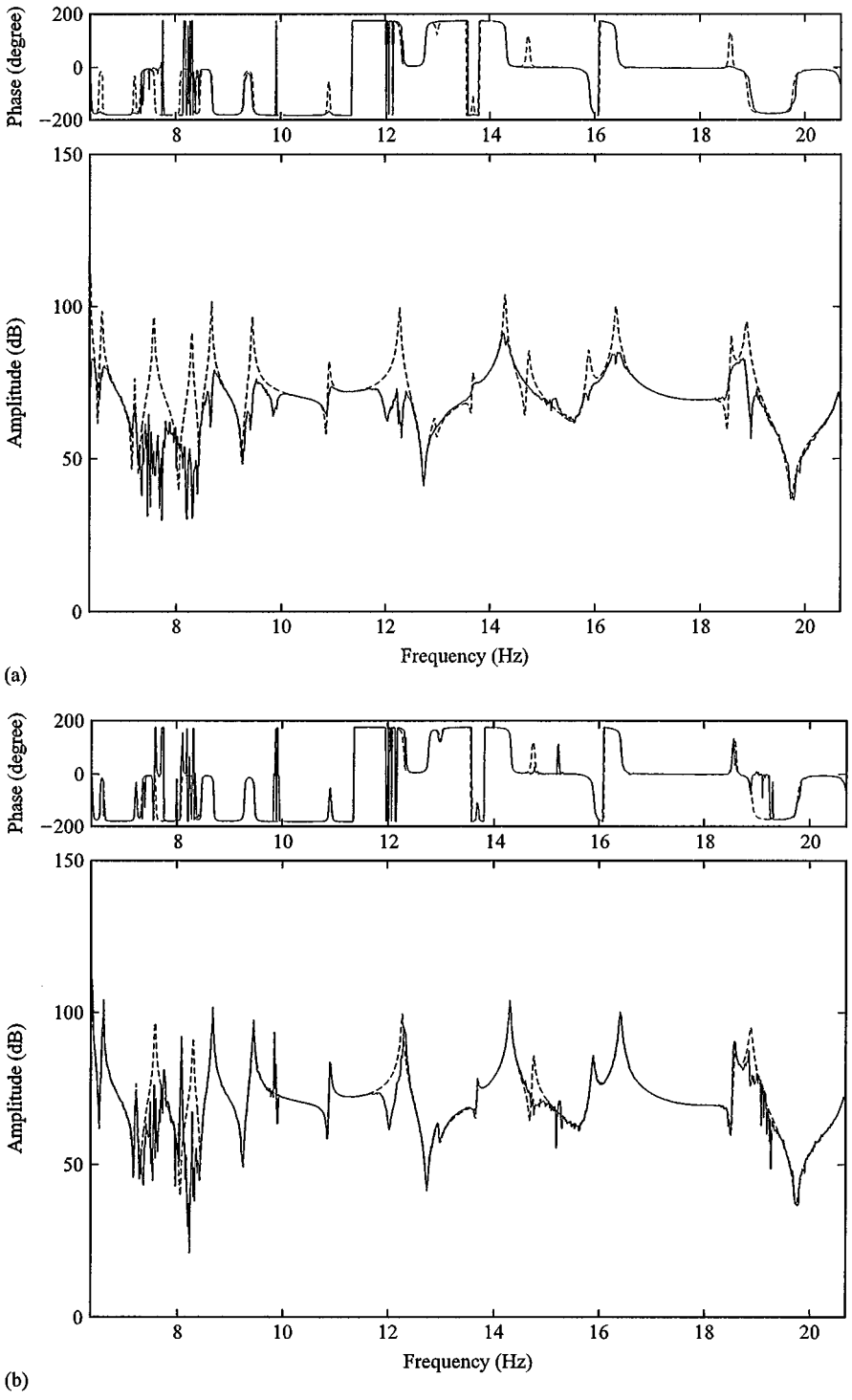


Figure 5. Comparison of exact and predicted system response functions (dB re. $10^{-5}$ m/s$^2$/N) of the two-component lumped parameter model applying LS and TLS algorithms with $m = 200$: (a) LS solution scheme (–––, exact; ——, prediction) and (b) TLS solution scheme (–––, exact; ——, prediction).

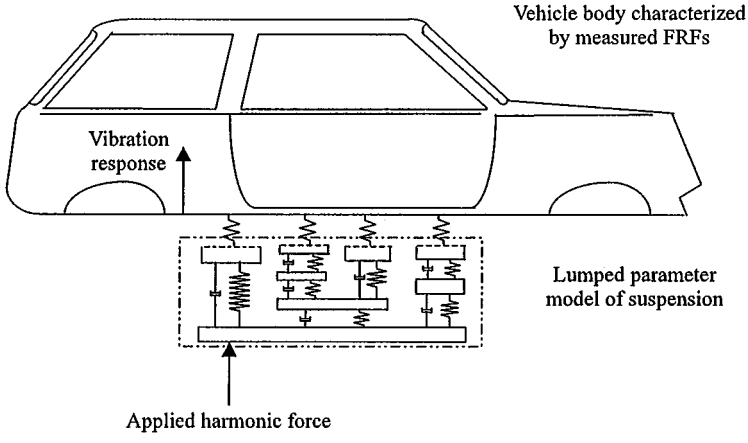


Figure 6. A practical example problem of a vehicle system body attached to a model of a suspension component at four discrete coupling positions. The problem is to compute the vibratory response of a point on the body due to applied force on the suspension.

distortion in the spectral curve. In addition, the calculation continues to generate spurious peaks that have no relation to the actual dynamic response which is highly misleading. On the other hand, the LS solution given by Figure 7(b) clearly provided a better overall estimate of the system response due to the inherent spectral-averaging effect. The slight deviation from the exact response curve observed is due to the influence of bias error that cannot be minimized by the least-squares calculation. To illustrate this limitation, consider the LS solution to the problem $[A][X] + [\varepsilon] = [B]$, where $[\varepsilon]$ is a residual matrix, given by $[X_{LS}] = ([A]^H[A])^{-1}[A]^H[B]$ that is also discussed in reference [14]. For pure random error, the expected value of $[\varepsilon]$ is zero, but this is not the case when a bias error exists. Substitution for $[B]$ in the $[X_{LS}]$ expression leads to $[X_{LS}] = [X] + ([A]^H[A])^{-1}[A]^H[\varepsilon]$, which clearly shows a difference between the computed $[X_{LS}]$ and exact $[X]$ if $[\varepsilon]$ is non-zero.

## 4. ERROR REDUCTION USING TSVD

### 4.1. THEORY

In the previous section, we have shown that the LS and TLS solution schemes are superior to the standard direct inverse algorithm when both are applied to an over-determined algebraic problem posed by equation (4). In spite of this improvement, there are still limitations in these two approaches as illustrated in Figure 5 and 7. To further increase the accuracy of the FRF-based dynamic coupling computations in the presence of error in FRFs, the TSVD scheme is proposed to enhance the precision of both LS and TLS algorithms.

The TSVD theorem permits one to nullify the smallest $n - k$ singular values where $[\Lambda_k] = \text{diag}(s_1, s_2, \ldots, s_k, 0, \ldots, 0)$ for $k < n$ and remove them from the problem such that the lower rank matrix $[A_k] = [U][\Lambda_k][V]^H$ provides the best

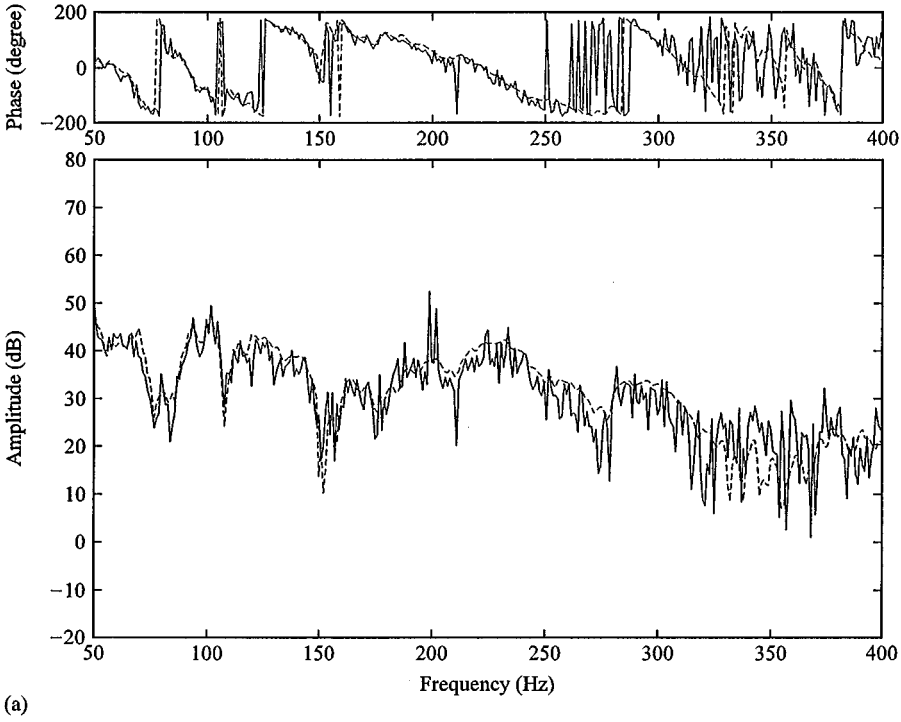


(a)

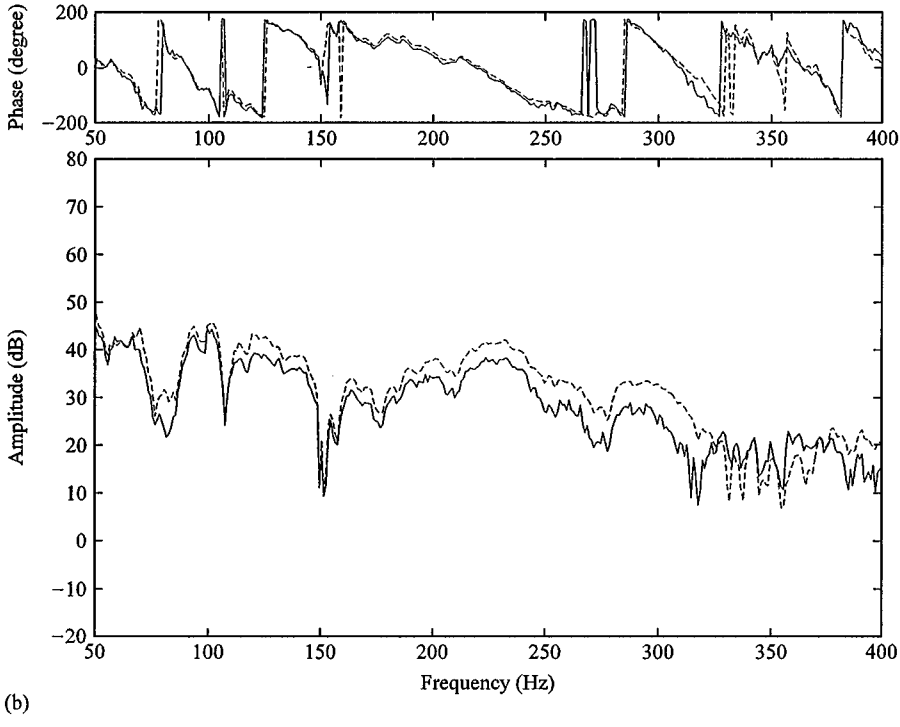


(b)

Figure 7. Comparison of exact and predicted system response functions (dB re. $10^{-5}$ m/s$^2$/N) of the vehicle system applying the (a) standard direct inverse scheme (–––, exact; ——, prediction) and (b) least square with $m = 80$ (–––, exact; ——, prediction).

approximation to $[A]$ in the sense of the Frobenious norm among all possible matrices of rank $k$. Thus, the Moore–Penrose pseudo-inverse of $[A_k]$ is $[A_k]^+ = [V][\Lambda_k]^+[U]^H$, where $[\Lambda_k]^+ = \text{diag}(1/s_1, 1/s_2, \ldots, 1/s_k, 0, \ldots, 0)$. As studied previously in references [7, 8], there are two fundamental ways to apply the singular value truncation described above in the FRF-based dynamic coupling equation. One approach is to eliminate the insignificant singular values of the "virtual" system compliance matrix expressed as $[H_{ii1}] + [H_{ii2}]$. In this case, its theoretical TSVD solution is given by $[X_k] = [A_k]^+[H_{iip}] = [V][\Lambda_k([A])]^+[U]^H[H_{iip}]$. Similarly, the TSVD solution for the noisy field (with error contamination in the FRFs) is given by $[\tilde{X}_k] = [\tilde{V}][\tilde{\Lambda}_k([\tilde{A}])]^+[\tilde{U}]^H[\tilde{H}_{iip}]$. Then unless $\sum_{g=k+1}^{n}(1/s_g([A])\sqrt{\sum_{j=1}^{n}([U]^H[H_{iip}])_{gj}^2}$ is small enough, $\|[X] - [X_k]\|_F$ is indispensable compared to $\|[H_{iip}]\|_F$, where $[X]$ represents the exact solution and the subscript $F$ refers to the Frobenious norm. Hence, applying TSVD to matrix $[A]$ of equation (4) could result in significant loss of important dynamic information. This problem was also noticed and briefly mentioned by Otte *et al.* [9] but without any theoretical proof like the one provided here.

The alternative approach is to apply TSVD to $[H_{iip}]$ directly. This is a result of realizing that $[H_{iip}]$ is the only matrix term in equation (4) that is corrupted by error but it is also present on both sides of the algebraic equality. To evaluate the effectiveness of this proposed idea, three different solution schemes are analyzed: (1) the exact solution to the idealized problem of $([H_{iip}] + [H_{iiq}])[X] = [H_{iip}]$ $(p \neq q)$ where no error is present; (2) LS or TLS solution of $([H_{iiq}] + [\tilde{H}_{iip}]_k)$ $[\tilde{X}]_k = [\tilde{H}_{iip}]_k$ where $k = n$ and $p$ refers to the specific component with inaccuracies in its FRFs; and (3) TSVD-based LS and TLS solutions of $([H_{iiq}] + [\tilde{H}_{iip}]_k)[\tilde{X}]_k = [\tilde{H}_{iip}]_k$ where $k < n$ and $[\tilde{H}_{iip}]_k$ is composed of only singular values not less than $\bar{s}_k$ and their corresponding $\tilde{u}_i$ and $\tilde{v}_i$ of $[\tilde{H}_{iip}]$. By comparing the latter two solutions to the first one, the effect of TSVD when applied to $[\tilde{H}_{iip}]$ can be evaluated conclusively.

First let $[A] = [H_{iiq}] + [H_{iip}]$ and $[\tilde{A}_k] = [H_{iiq}] + [\tilde{H}_{iip}]_k$ for $p \neq q$, then the LS solution to $([H_{iiq}] + [\tilde{H}_{iip}]_k)$ $[\tilde{X}]_k = [\tilde{H}_{iip}]_k$ is

$$[\tilde{X}_{LS}]_k = ([\tilde{A}_k]^H[\tilde{A}_k])^{-1}[\tilde{A}_k]^H[\tilde{H}_{iip}]_k \tag{9}$$

and thus the difference between the LS and exact theories is given by

$$[\tilde{X}_{LS}]_k - [X] = ([\tilde{A}_k]^H[\tilde{A}_k])^{-1}[\tilde{A}_k]^H[\tilde{H}_{iip}]_k - ([A]^H[A])^{-1}[A]^H[H_{iip}]. \tag{10}$$

Substituting $[\tilde{H}_{iip}]_k = [H_{iip}] + [E] - [T_k]$ into the above equation, where $[E]$ is the matrix representing the error in $[H_{iip}]$ and $[T_k]$ is the truncated matrix given by $\sum_{j=k+1}^{n} \tilde{s}_j([H_{iip}])\tilde{u}_j\tilde{v}_j^H$, directly gives

$$\begin{aligned}[\tilde{X}_{LS}]_k - [X] = {} & ([\tilde{A}_k]^H[\tilde{A}_k])^{-1}([A]^H[A] - [\tilde{A}_k]^H[\tilde{A}_k]) \\ & \times ([A]^H[A])^{-1}[A]^H[H_{iip}] \\ & + ([\tilde{A}_k]^H[\tilde{A}_k])^{-1}[([E] - [T_k])^H[H_{iip}] + [A]^H \\ & \times ([E] - [T_k]) + ([E] - [T_k])^H([E] - [T_k])].\end{aligned} \tag{11}$$

Equation (11) can be simplified by rearranging similar terms and substituting for $[A][X] = [H_{iip}]$ to get

$$[\tilde{X}_{LS}]_k - [X] = ([\tilde{A}_k]^H[\tilde{A}_k])^{-1}[\tilde{A}_k]^H([E] - [T_k])([H_{iip}]^H[H_{iip}])^{-1} \times [H_{iip}]^H[H_{iiq}][X]. \tag{12}$$

Then, taking the norms of both sides of equation (12) yields two closed-form conditions

$$L^{(1)}_{LS,k} \leqslant \|[\tilde{X}_{LS}]_k - [X]\|_F \leqslant L^{(n)}_{LS,k}, \tag{13a}$$

$$L^{(j)}_{LS,k} = \frac{\|([E] - [T_k])([H_{iip}]^H[H_{iip}])^{-1}[H_{iip}]^H[H_{iip}][X]\|_F}{\tilde{s}_j([\tilde{A}_k])}, \quad j = 1, n, \tag{13b}$$

By comparison, the TLS solution is given by

$$[\tilde{X}_{TLS}] = ([\tilde{A}_k]^H[\tilde{A}_k] - (\tilde{s}'_{n+1})^2[I_n])^{-1}[\tilde{A}_k]^H[\tilde{H}_{iip}]_k, \tag{14}$$

where $\tilde{s}'_{n+1}$ is the $(n+1)$th singular value of $[([H_{iiq}] + [\tilde{H}_{iip}]_k)\,[\tilde{H}_{iip}]_k]$. Similar to the derivation of equation (12), the difference between this approximate solution and the exact one is given by

$$[\tilde{X}_{TLS}]_k - [X] = ([\tilde{A}_k]^H[\tilde{A}_k] - (\tilde{s}'_{n+1})^2[I_n])^{-1}[W], \tag{15a}$$

$$[W] = ([\tilde{A}_k]^H([E] - [T_k])([H_{iip}]^H[H_{iip}])^{-1}[H_{iip}]^H[H_{iiq}] + (\tilde{s}'_{n+1})^2[I_n])[X], \tag{15b}$$

with the Frobenious norm expressed in closed form as

$$L^{(1)}_{TLS,k} \leqslant \|[\tilde{X}_{TLS}]_k - [X]\|_F \leqslant L^{(n)}_{TLS,k}, \tag{16a}$$

$$L^{(j)}_{TLS,k} = \frac{\|([\tilde{A}_k]^H([E] - [T_k])([H_{iip}]^H[H_{iip}])^{-1}[H_{iip}]^H[H_{iiq}] + (\tilde{s}'_{n+1})^2[I_n])[X]\|_F}{\tilde{s}_j([\tilde{A}_k]^H[\tilde{A}_k] - (\tilde{s}'_{n+1})^2[I_n])}, \quad j = 1, n. \tag{16b}$$

For any given set of conditions, the smaller the Frobenious norm of $[\tilde{X}_k] - [X]$, the better is the estimation $[\tilde{X}_k]$ of $[X]$. Also, if there exist a $k \neq n$ such that $L^{(n)}_k < L^{(1)}_n$, the dynamic coupling result of either the enhanced LS or TLS scheme based on applying TSVD to $[\tilde{H}_{iip}]$ is guaranteed to match the theoretical response better than the direct calculations due to the fact that $\|[\tilde{X}_k] - [X]\|_F < \|[\tilde{X}_n] - [X]\|_F$. Although equations (13) and (16) give the explicit expressions of the upper and lower boundaries of $\|[\tilde{X}_k] - [X]\|_F$, in practice one can only compute $[\tilde{A}_k]$, $[T_k]$ and the corresponding singular values. The matrix parameter given by $[E]$ is usually difficult to estimate without prior knowledge of the source of error and thus makes it quite difficult to compute the boundary values precisely. However, for a specific class of restricted problem, a comprehensive set of database can be developed for the purpose of estimating $[E]$ more precisely in new but related cases.

From equations (13) and (16), it can be seen clearly than the singular values $\tilde{s}_i([\tilde{A}_k])$ and $\tilde{s}_i([\tilde{A}_k]^H[\tilde{A}_k] - (\tilde{s}'_{k,n+1})^2[I_n])$ for $i = 1$ and $n$, play a significant role in determining $\|[\tilde{X}_k] - [X]\|_F$. Thus, it is desirable to understand how they vary with $k$ when TSVD is applied. According to reference [15], if $[B_q]$, $[B_p]$ and $[E_B]$ are $m \times n$ matrices satisfying the equality of $[B_q] - [B_p] = [E_B]$, then their respective singular values given by $\beta_{q,i}, \beta_{p,j}$ and $\varepsilon_i, i = 1, 2, \ldots, J$, where $J = \min(m, n)$, must satisfy the inequality $|\beta_{q,i} - \beta_{p,i}| < \varepsilon_1 \equiv \|[E_B]\|_2$. Applying this theorem to the current TSVD-based LS problem, where $[\tilde{A}_n] - [\tilde{A}_k] = [T_k]$, directly yields the inequality

$$|\tilde{s}_i(\tilde{A}_n) - \tilde{s}_i(\tilde{A}_k)| < \tilde{s}_k(\tilde{H}_{iip}). \tag{17}$$

The above equation actually reflects how the proposed TSVD scheme influences the approximate "virtual" system compliance matrix, $[\tilde{A}_k] = [H_{iiq}] + [\tilde{H}_{iip}]_k$. If the largest neglected singular value of $[\tilde{H}_{iip}]$ is relatively significant compared to $\tilde{s}_n([\tilde{A}_n])$, then the difference between $\tilde{s}_n([\tilde{A}_n])$ and $\tilde{s}_n([\tilde{A}_k])$ may be quite large. Accordingly, one can simply examine $\tilde{s}_n([\tilde{A}_k])$ from among $k = 0, 1, 2, \ldots, n$, and select the highest $\tilde{s}_n([\tilde{A}_k])$ that minimizes the upper boundary $L^{(n)}_{LS,k}$. But when the difference between $\tilde{s}_n([\tilde{A}_n])$ and $\tilde{s}_n([\tilde{A}_k])$ is small, the boundaries of $\|[\tilde{X}_{LS}]_k - [X]\|_F$ for different $k$ are mainly determined by the Frobenious norm in equations (13b) and (16b). Similar concluding remarks can be made for the boundaries of the TLS solution.

Further detailed examination of equations (13) and (16) also reveals other criteria for minimizing the Frobenious norm. For instance, this may be achieved if $([E] - [T_k])$ is approximately orthogonal to $([H_{iip}]^H[H_{iip}])^{-1}$ or $[\tilde{A}_k]$ even though it is not as common and is fairly difficult to compute. On the other hand, if $[T_k] \approx [E]$ in which the truncated part becomes nearly the same as the error norm, it is likely that the Frobenious norm can be minimized. To find the precise relationship between $[T_k]$ and $[E]$, first consider $[E_U] = [\tilde{U}_{iip}] - [U_{iip}]$, $[E_V] = [\tilde{V}_{iip}] - [V_{iip}]$ and $[E_S] = [\tilde{\Lambda}_{iip}] - [\Lambda_{iip}]$. Also, let $[\Lambda_{iip}] = [\Lambda_{iip,a}] + [\Lambda_{iip,b}]$, where $[\Lambda_{iip,a}] = \text{diag}(s_1, s_2, \ldots, s_k, 0 \cdots 0)$ and $[\Lambda_{iip,b}] = \text{diag}(0 \cdots 0, s_{k+1}, \ldots, s_n)$. Similarly, it can be shown that $[\tilde{\Lambda}_{iip}] = [\tilde{\Lambda}_{iip,a}] + [\tilde{\Lambda}_{iip,b}]$ and the error matrix is

$$[E] = [\tilde{H}_{iip}] - [H_{iip}] = [\tilde{U}_{iip}][\tilde{\Lambda}_{iip}][\tilde{V}_{iip}]^H - [U_{iip}][\Lambda_{iip}][V_{iip}]^H. \tag{18}$$

Substituting the differential matrices into equation (18) and ignoring higher order terms lead to the following approximation for the error matrix:

$$\begin{aligned}[E] \approx\ & [E_U](\Lambda_{iip}] - [\tilde{\Lambda}_{iip,b}])[V_{iip}]^H + [U_{iip}]([\Lambda_{iip}] - [\tilde{\Lambda}_{iip,b}])[E_v]^H \\ & + [U_{iip}]([\tilde{\Lambda}_{iip,a}] - [\Lambda_{iip,a}])[V_{iip}]^H - [U_{iip}][\Lambda_{iip,b}][V_{iip}]^H \\ & + [\tilde{U}_{iip}][\tilde{\Lambda}_{iip,b}][\tilde{V}_{iip}]^H. \end{aligned} \tag{19}$$

Note that the last term in the above equation is simply the truncated matrix of $[T_k]$. Hence, it is obvious that the influence of error can be reduced significantly if

$[T_k]$ dominates $[E]$. This is satisfied whenever the sum effect of the first four terms in equation (19) vanishes. Since this requirement is far to complex to be practical, we can only discuss certain special cases where each of the first four items is small compared to $[E]$. This leads to a sufficient but not necessary condition for $[E] \approx [T_k]$.

First, consider the case in which the differential matrices are relatively small implying that $[U_{iip}]$ and $[V_{iip}]$ do not vary significantly. Hence, the first two terms related to $[E_U]$ and $[E_V]$ can be neglected. The third term vanishes only if $[\tilde{\Lambda}_{iip,a}] \approx [\Lambda_{iip,a}]$ and the fourth term of the unperturbed matrix $[U_{iip}]$ $[\Lambda_{iip,b}][V_{iip}]^H$ is small if $[\Lambda_{iip,b}] \approx 0$, which means that the truncated part is not the primary component of $[H_{iip}]$. The scenario mentioned above suggests that our proposed TSVD scheme will be effective when the truncated singular value $s_i$ is not only small and plays a minor role in the composition of $[H_{iip}]$ but is the only term affected significantly by the discrepancies in the FRFs.

### 4.2. NUMERICAL EXAMPLE

The previous two examples discussed in section 3 are re-examined here. By comparing the predictions of $[\tilde{H}_{iip}]_k$ for $k = 1, 2, \ldots, n$ using the enhanced TSVD-based least-squares approaches to the exact solution, the best estimator of $[X]$ can be obtained. For the lumped parameter model, typical response functions from the enhanced LS and TLS solution schemes are shown in Figures 8(a, b) respectively. Here, the computations produce considerable improvement over the previous direct inverse calculation shown in Figure 3(b). Even in the frequency range of 2–10 Hz where the influence of error was quite significant before, the best estimator of the enhanced solutions found by applying the above criteria now produces much more accurate results. The response function predicted by the enhanced LS algorithm improves significantly at the off-resonance regime and gets closer to the exact amplitude of the resonance peaks. The predictions of the TLS counterpart are even more precise than the enhanced LS results, although some differences can still be seen. This discrepancy is inevitable because the influence of error cannot be completely discarded since some percentage of the errors is inter-mingled with the actual dynamics.

A similar quality of improvement in the predicted result was also seen in the second more realistic vehicle example where the body component is represented by measured FRFs depicting higher damped modal density characteristic. A typical comparison of coupled system response spectra is shown in Figure 9. Compared to the results in Figure 7, the predicted response curve based on applying TSVD to the least-squares solution is significantly closer to the exact response curve. This is because the influence of bias error is also reduced to some extent since the proposed TSVD scheme can inherently deal with both random and bias errors simultaneously. Again, the slight deviation that still exists in the calculation is partly attributed to the fact that the FRF errors are inter-mingled with the low-level dynamic response of the structural component. Hence, the effect of reducing the FRF error amplification from the pseudo-inverse calculation also resulted in the loss of some dynamic information, which cannot be avoided.

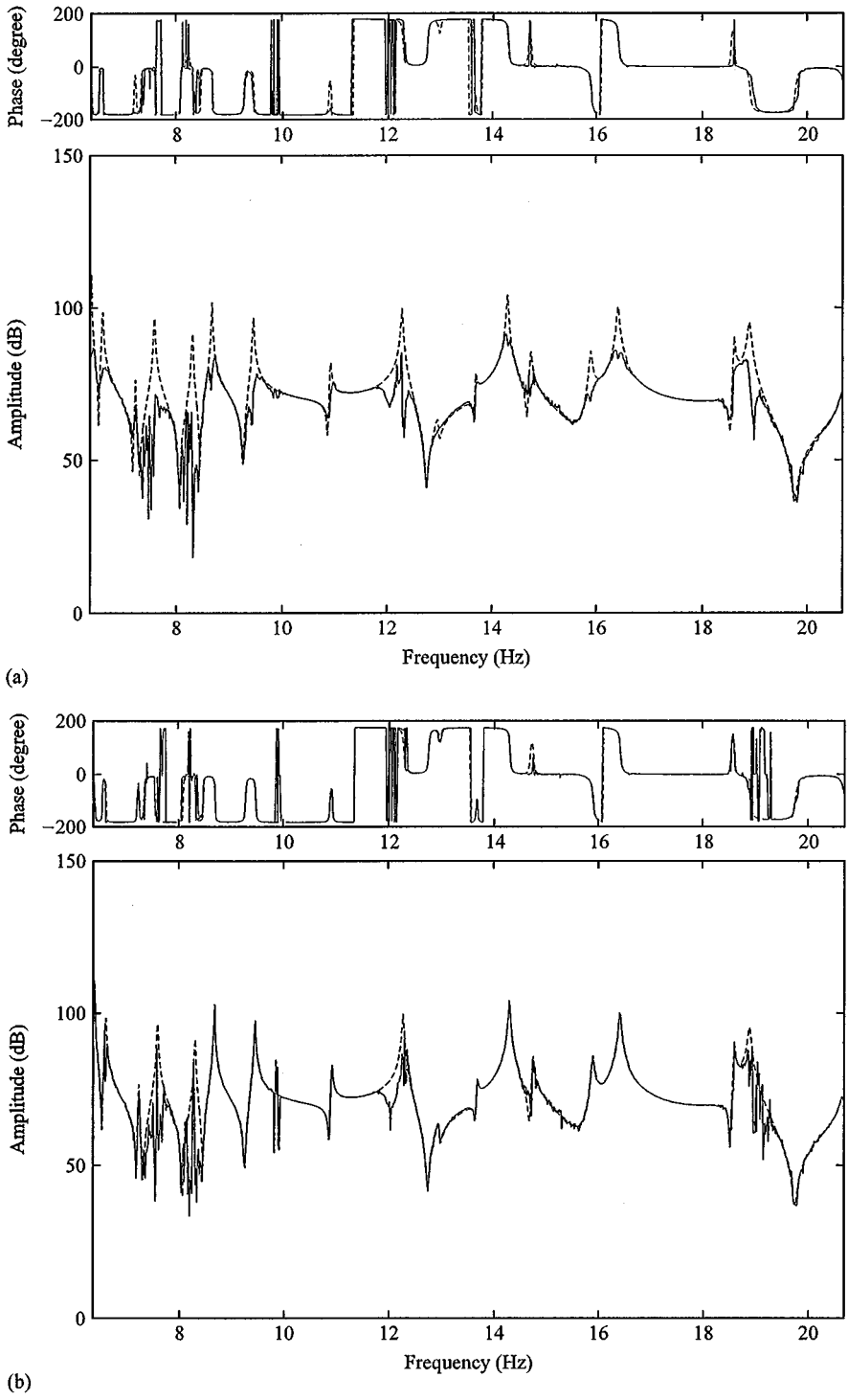


Figure 8. Comparison of exact and enhanced predictions of system response functions (dB re. $10^{-5}$ m/s$^2$/N) of the lumped parameter model applying the combined TSVD and least-squares approaches: (a) with enhanced LS (---, exact; ——, prediction) and (b) with enhanced TLS (---, exact; ——, prediction).

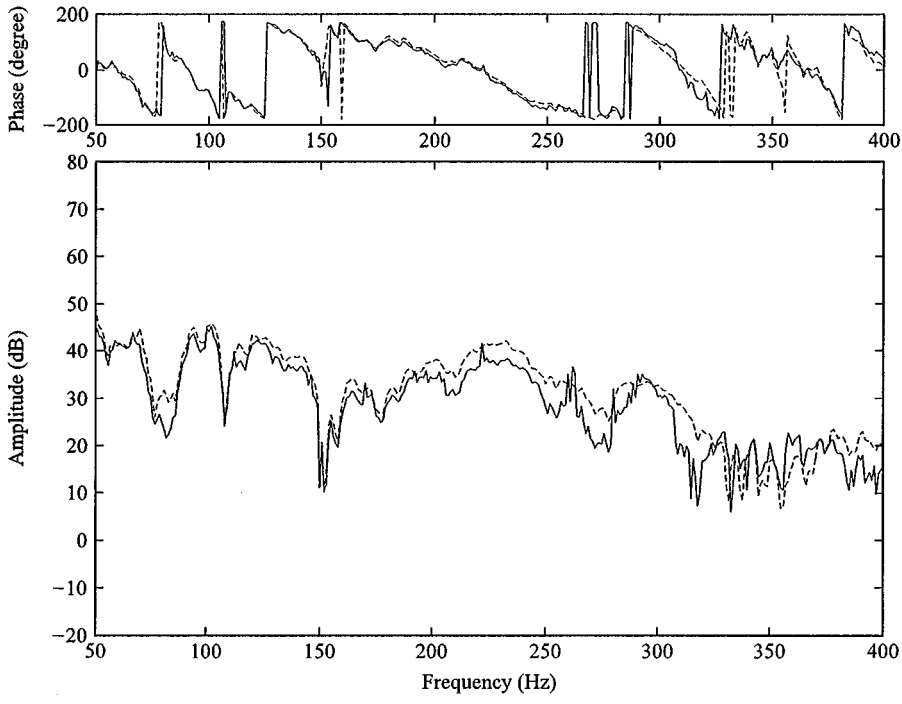


Figure 9. Comparison of exact and enhanced predictions of system response functions (dB re. $10^{-5}$ m/s$^2$/N) of the vehicle system by applying the combined TSVD and least-squares approaches (---, exact; ——, prediction).

The above computation results show that when TSVD is applied appropriately to enhance the least-squares approaches, it is possible to minimize the influence of the FRF error and thereby recover the overall coupling results almost precisely. On the other hand, careless application of TSVD can result in poorer predictions. For instance, if the two smallest singular values of $[H_{iip}]$ are just simply truncated over the entire frequency range of interest in the vehicle example, the predicted system response spectrum for the same point on the body structure becomes distorted as shown in Figure 10. This discrepancy is more evident and worse at higher frequencies.

## 5. CONCLUDING REMARKS

The numerical deficiency that inherently exists in the FRF-based component synthesis approach has been examined theoretically and computationally in this paper. The standard inverse calculation that is part of the spectral formulation of this method has been reformulated and posed as the problem of analyzing the numerical stability of an over-determined set of linear algebraic equations. This transformation resulted in a new formulation that possesses many advantages over the direct approach, and had not been proposed in the past. It is first shown that the solution to this problem can be improved by applying either the LS or TLS

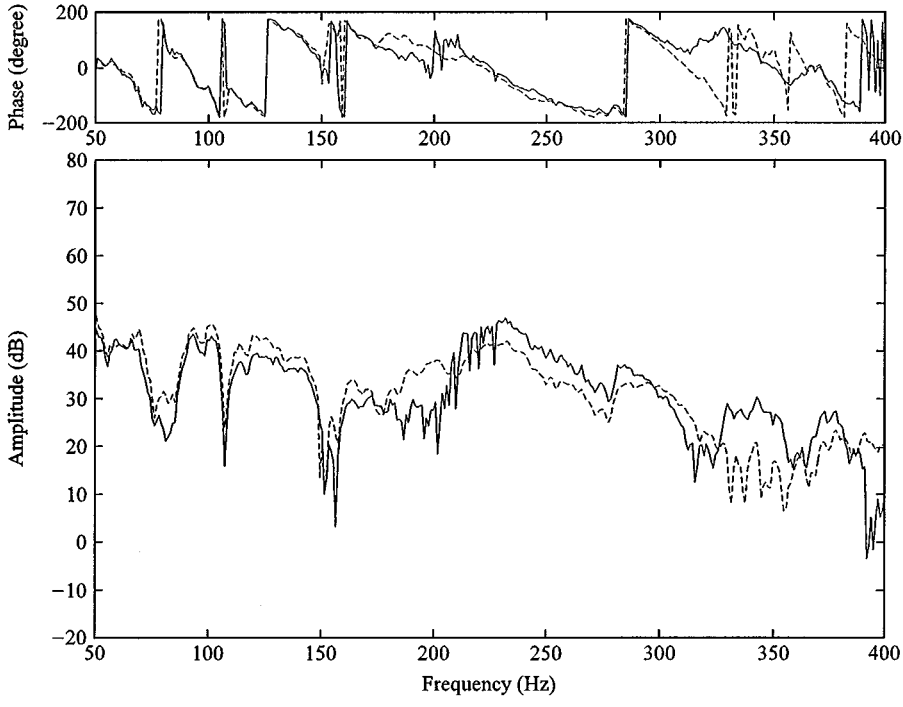


Figure 10. Distortion in the predicted system response (dB re. $10^{-5}$ m/s$^2$/N) of the vehicle system due to arbitrary truncation of the two least-significant singular values uniformly over the entire frequency range of interest (---, exact; ——, prediction).

algorithm to take advantage of the spectral-averaging effect that involves more than one set of FRF-matrix. To further improve the dynamic coupling computational accuracy, the combined TSVD and least-squares approach is proposed. The theoretical basis for the effectiveness of TSVD has been examined by explicitly deriving the boundary limits for the deviation of the estimated solution from its exact theoretical value. From the explict expression of the difference between exact theoretical response and approximate computational solution, specific conditions affecting the accuracy of TSVD were examined. First, it is sufficient for the truncated part of the error-corrupted compliance matrix to be close to the actual error matrix, which is difficult to verify in practice. The other more tangible criterion that depends on finding the largest $\tilde{s}_n([\tilde{A}_k])$ and $\tilde{s}_i([\tilde{A}_k]^H[\tilde{A}_k] - (\tilde{s}'_{k,n+1})^2[I_n])$ in the LS and TLS schemes, respectively, provides a guideline for selecting the proper $k$ value. On the other hand, actual dynamic information will be lost if non-negligible singular values are nullified resulting in inadequate system response functions. Finally, the effectiveness and limitations of the FRF-based substructuring technique applying enhanced least-squares and TSVD approaches are applied quite successfully to two numerical examples involving a multi-degrees-of-freedom lumped parameter model and an actual vehicle system. Further, applied research is needed to quantify the limitations and extensions of this proposed approach for more complex structures to better define

the optimal criterion for the TSVD filtration and understand the effect of filtering on different classes of structural modes.

## REFERENCES


1. W. C. Hurty 1965 *Journal of the American Institute of Aeronautics and Astronautics* **3**, 678–685. Dynamic analysis of structural system using component modes.
2. R. Craig and M. C. Bampton 1968 *Journal of the American Institute of Aeronautics and Astronautics* **6**, 1313–1319. Coupling of substructures for dynamic analysis.
3. D. J. Ewins 1984 *Modal Testing*: *Theory and Practice*. New York: Research Studies Press Ltd.
4. S. D. Ochsner and R. J. Bernhard 1995 *Noise Control Engineering Journal* **43**, 73–82. Application of a component mobility technique to automotive suspension systems.
5. T. C. Lim 1996 *Noise Control Engineering Journal* **44**, 245–248. Case history: finite element and experimental modeling approaches for automotive noise control problems.
6. T. C. Lim and G. C. Steyer 1992 *Journal of Passenger Cars* **101**, 585–591. Hybrid experimental–analytical simulation of structure-borne noise and vibration problems in automotive systems.
7. T. C. Lim and G. C. Steyer 1991 *Proceedings of the Ninth International Modal Analysis Conference*, 902–908. An improved numerical procedure for the coupling of dynamic components using frequency response functions.
8. D. Otte, J. Leuridan, H. Grangier and R. Aquilina 1990 *Proceedings of the Eighth International Modal Analysis Conference*, 213–220. Coupling of structures using measured FRF's by means of SVD-based data reduction techniques.
9. D. Otte, J. Leuridan, H. Grangier and R. Aquilina 1991 *Proceedings of the Ninth International Modal Analysis Conference*, 909–918. Prediction of the dynamics of structural assemblies using measured FRF-data: some improved data enhancement techniques.
10. M. S. Kompella and R. J. Bernhard 1997 *Noise Control Engineering Journal* **45**, 133–142. Techniques for prediction of the statistical variation of multiple–input–multiple-output system response.
11. M. S. Kompella 1992 *Ph.D. dissertation*, *Purdue University*. Improved multiple-input/multiple-output modeling procedures with consideration of statistical information.
12. J. M. Varah 1973 *SIAM Journal of Numerical Analysis* **10**, 257–267. On the numerical solution of ill-conditioned linear systems with applications to ill-posed problems.
13. R. E. Powell 1983 *Ph.D. dissertation*, *MIT*. Multichannel inverse filtering of machinery vibration signals.
14. M. G. Kendall and A. Stuart 1979 *The Advanced Theory of Statistics*. London: Griffin, fourth edition.
15. C. L. Lawson and R. J. Hanson 1974 *Solving Least Squares Problems*. Englewood Cliffs, NJ: Prentice-Hall, Inc.
16. G. H. Golub and C. F. Van Loan 1996 *Matrix Computations*. Baltimore: Johns Hopkins University Press.
17. G. H. Golub and C. F. Van Loan 1980 *SIAM Journal of Numerical Analysis* **17**, 883–893. An analysis of the total least squares problem.
18. S. Van Huffel and J. Vandewalle 1989 *Numerical Math.* **55**, 431–449. Algebra connection between the least squares problems.


## APPENDIX A: NOMENCLATURE

| | |
|---|---|
| $s$ | singular value |
| $E$ | error matrix |

| | |
|---|---|
| $F$ | force |
| $H$ | compliance |
| $I_n$ | $n \times n$ identity matrix |
| $K$ | stiffness |
| $L$ | boundary limit |
| $T$ | truncated matrix |
| $U$ | left unitary matrix of singular value decomposition |
| $V$ | right unitary matrix of singular value decomposition |
| $\Lambda$ | singular value matrix |

*Subscripts and superscripts*

| | |
|---|---|
| $e$ | excitation co-ordinate |
| $i$ | interface coupling co-odrinate |
| $k$ | singular value number |
| $m, n$ | dimensions of matrices |
| $p, q$ | component labels |
| $r$ | response co-ordinate |
| $F$ | Frobenious norm |
| $H$ | Hermitian transpose |
| $II$ | second norm of a vector |
| $S$ | system |
| $\sim$ | matrix with error |
| $+$ | Moore–Penrose pseudo-inverse |